MODELING THE CONTINUOUS PRESSING PROCESS FOR WOOD-BASED COMPOSITES

Heiko Thoemen

Assistant Professor
Department of Wood Science and Technology
University of Hamburg, Leuschnerstrasse 91
21031 Hamburg, Germany

and

Philip E. Humphrey

Associate Professor
College of Forestry
Oregon State University
Corvallis, OR 97331-7402

(Received July 2002)

ABSTRACT

The quantitative and economical importance of continuous pressing has increased steadily over the last two decades. An analytical model will be helpful in better understanding and improving this process and in developing new manufacturing techniques. Reported here is a simulation model that accounts for heat and mass transfer as well as rheological and adhesion mechanisms that occur in three dimensions as mat material passes through a continuous press. The model enables one to predict the evolution of important variables including temperature, moisture content, air and water vapor pressure, density profile, and adhesive bond strength. The scientific principles upon which the model depends are summarized along with the boundary conditions and modeling strategy employed. Model predictions are presented and discussed for a typical medium density fiberboard (MDF) production plant.

Keywords: Wood-based composites, continuous pressing, computer simulation, thermodynamics, rheology, adhesion, density profile development, product and process innovations.

BACKGROUND

During the consolidation of wood-furnish mats in hot presses, a wide range of events occurs simultaneously. The most important are heat transfer and flow of gas mixtures, phase change of water, densification of the material, development of internal stresses, and adhesive cure. Fundamental knowledge about these mechanisms and their interaction is essential to improving our understanding of the pressing process. Such understanding is necessary for optimization of existing production processes and for the development of new products and techniques for their production.

The effects of many material and pressing parameters on panel properties and production speed have been addressed in the past, with the majority of these studies being empirical. The determination of simple links between single production and output parameters is, however, made difficult by the complexity of interactions among almost all individual mechanisms.

In order to develop a scientifically based method to quantify the impact of variations in pressing conditions on the process and final product, some researchers have proposed an integrated approach that considers those variables important during hot pressing simultaneously rather than in isolation. Among the first were Kavvouras (1977) and Bolton and Humphrey (1988). This approach, along with the rapid increase of computational power, laid the foundation on which to develop analytical process models based on fundamental principles.

A few analytical models of hot pressing have been presented during the last two decades. Thoemen (2000) gives a comprehensive literature review of such models. All models published to date simulate batch presses. Continuous pressing has, however, been increasing steadily in quantitative and economical importance. Not only does the productivity of this technology exceed that of batch pressing, but it also has opened new opportunities to manipulate panel properties.

Existing models for batch presses can be extrapolated to the continuous press to a certain degree, the physical mechanisms within the mat being the same in both types of machine, but there are serious limitations to so doing. Not all of the important features of continuous pressing can be simulated by modifying conventional models of the batch pressing process. In the continuous press, for example, the boundary conditions change in the feed direction. Furthermore, the gas mixture in the continuous press escapes not only through the sides of the mat, but also through its surfaces immediately in front of and behind the press.

The model presented here can be applied to both batch and continuous pressing processes; it is summarized in this paper, with those aspects that are specific to the continuous press presented in more detail. The interested reader is referred to Thoemen and Humphrey (2003a, b) for a comprehensive description of the basics of the model and the numerical procedures employed. Predictions of interfiber bond strength development, based on adhesion kinetics data derived with the ABES technique (Humphrey 1999), are not included here; they will be dealt with in a separate publication.

MODELING MASS AND HEAT TRANSFER AND RHEOLOGY

The model consists of a three-dimensional heat and mass transfer model, combined with a one-dimensional rheological model. Both components will be summarized in turn; derivations and justifications of model assumptions and mathematical formulations are not included here; they are dealt with in Humphrey and Bolton (1989a), Thoemen and Humphrey (2003a, b), and Thoemen (2000).

For modeling purposes, the wood-furnish mat is considered as a homogeneous material. That is to say, a macroscopic view is used where the size of the representative volume is large relative to that of the wood constituents. However, a microscopic view is used whenever appropriate to illustrate model assumptions or to explain specific features of the modeled system.

Summary of mass and heat transfer mechanisms

The wood-furnish mat is a capillary-porous material consisting of natural fiber cell wall material and inter- and intra-particle voids, which form a system of interlinked cavities. The gas in the pore spaces is regarded as a pure two-component mixture of air and water vapor. Measurements reported by Denisov et al. (1975) suggest that the proportion of other components is relatively small; their influence on the gas properties and mass and heat transfer rates is therefore unlikely to be significant. Future versions of the model will, however, account for the generation and movement of substances such as volatile organic compounds and formaldehyde, since these may be environmentally important and may play roles in the kinetics of adhesive cure or chemical modification of fibers.

The model accounts for three-dimensional convective and diffusive gas flow through the void system of the mat. Bound water diffusion, surface diffusion, and the translation of water condensed in small inter-particle capillaries are unlikely to be significant relative to water vapor translation through the void system; they are not included, therefore, in the model.

Convective fluxes of the gas mixture develop in response to total gas pressure gradients and can be calculated by applying Darcy's law. Total pressure gradients develop between the surfaces and the central plane of the mat and between its horizontal center and edges. While the horizontal gradients may be considerable, the cross-sectional ones usually dissipate almost instantaneously in particulate composites (Thoemen 2000). Darcy's law is used in the form:

$$j_i^c = -\frac{k_p}{\eta}\frac{M_i}{RT_{abs}}p_i\nabla p \qquad i = v, a \qquad (1)$$

where:

- v, a subscripts to denote vapor or air
- j_i^c convective flux of component i [kg m^{-2} s^{-1}]
- M_i molecular mass of component i [kg mol^{-1}]
- p_i partial pressure of component i [Pa]
- p total gas pressure [Pa]
- R gas constant [J mol^{-1} K^{-1}]
- T_{abs} absolute temperature [K]
- k_p permeability coefficient [m^2]
- η dynamic viscosity of the gas mixture [Pa s]

In addition, diffusive fluxes occur that are caused by partial pressure gradients of the gas components. This mechanism likely contributes little to overall mass transfer during hot pressing. Considerable partial pressure gradients of air and water vapor develop between the surfaces and the central plane of the mat however, at least temporarily. Diffusive fluxes can be described by Fick's law:

$$j_i^d = -D_{eff}\frac{M_i}{RT_{abs}}\nabla p_i \qquad i = v, a \qquad (2)$$

where:

- j_i^d diffusive flux of component i [kg m^{-2} s^{-1}]
- D_{eff} effective diffusion coefficient [m^2 s^{-1}]

Finally, to calculate the total flux j_i of component i, the diffusive flux may be superimposed on the convective flux:

$$j_i = j_i^d + j_i^c \quad i = v, a \qquad (3)$$

Both conductive and convective heat transfer in three dimensions are accounted for. Conductive heat fluxes are proportional to temperature gradients and can be described by Fourier's law:

$$q = -k_t\nabla T \qquad (4)$$

where:

- q conductive heat flux [J m^{-2} m^{-1}]
- k_t thermal conductivity [W m^{-1} K^{-1}]
- T temperature [°C or K]

Convective heat transfer is associated with the gas flow (including diffusion) through the mat. In principle, two mechanisms contribute to convective heat transfer. First, phase change of water always accompanies the release or consumption of latent heat of evaporation and latent heat of sorption. Second, gas that moves from a hot to a cold region releases sensible heat, just as cold gas takes up heat energy when moving into a warmer region. The contribution of the transfer of sensible heat to overall heat flow is small, however, because the mass of vapor and air is very small compared to the mass of wood and bound water. The transfer of sensible heat is therefore not included.

Two moisture phases are recognized: water bound in the cell-wall material and water vapor in the voids; free water is not considered in the present approach. The moisture is assumed to be uniformly distributed within single wood particles, and also in local equilibrium with the vapor phase in the surrounding voids. This assumption appears to be justified for small particles, such as single wood fibers. However, when moving to simulate materials with large particle sizes (e.g., strands), it may become necessary to revise this assumption. The relationship between equilibrium moisture content (EMC), within-void relative humidity, and temperature may be expressed by sorption isotherms or sorption isopsychrens (i.e., lines of equal relative humidity). Apparently, the most comprehensive set of such data available in the literature for conditions including those above 100°C and vapor pressures above ambience are the sorption isopsychrens presented by Engelhardt (1979), who supplemented his own measurements in the range between 110 and 170°C with measurements reported by Weichert (1963) for temperatures below 100°C. The curves presented by Engelhardt were extrapolated for temperatures up to 220°C by fitting a second order polynomial to the measured data, and were then represented in a look-up table with the relative humidity as dependent variable.

Energy associated with the transition of water from the bound to vapor states, or *vice versa,* is composed of the latent heat of sorption (from the bound to the liquid state) and the latent heat of evaporation (from the liquid to the gaseous state). In the present model, a formulation presented by Humphrey and Bolton (1989a) is used to relate the latent heat of sorption and evaporation to moisture content (MC) and temperature.

Physical properties of the mat and the gases within may vary with respect to both space and time. Most properties are highly dependent on the local conditions of the mat. In addition, variations of the transport properties (e.g., permeability, thermal conductivity, and obstruction factor) in the three principal directions are accounted for in the model. A complete list of these dependencies is given in Thoemen and Humphrey (2003a).

Densification and the development of internal stresses

The wood furnish undergoes both instantaneous and time-dependent deformation upon application of pressing load. Such material behavior may be illustrated and mathematically described by employing rheological models in which individual strain components are represented by simple elements (e.g., a spring or a dashpot) or by a combination of such elements.

The four-element Burgers model is frequently used in rheology to describe visco-elastic material behavior. The strain that develops when stress is applied to a pure visco-elastic material may be divided into elastic, delayed-elastic, and viscous components. However, irreversible changes of cell wall and mat structure that happen instantaneously upon loading are the dominant type of deformation during densification of wood-furnish materials. The Burgers model does not represent this type of deformation. To account for both the visco-elastic material behavior and the instantaneous but irreversible deformation, Ren (1991) working with Humphrey supplemented the Burgers model by adding a plastic and micro-fracture (PMF) element in series (Fig. 1a). A schematic of the stress-strain relationship as it may be described by this rheological modeling approach is displayed in Fig. 1b. According to Ren's (1991) definition, strain caused by PMF effects occurs only if the effective stresses exceed the yield strength of the microstructure; such deformation is not recoverable when the load is removed. The PMF element may be symbolized by a spring that operates only in one direction.

Each of the five elements of the enhanced Burgers model (hereafter referred to as the Burgers-Humphrey model) presented in Fig. 1a can be described by a rheological coefficient. These coefficients must be expressed as functions of temperature, MC, and density. Given the rheological coefficients and the effective stress, the local deformation of the wood furnish can be computed as the sum of the four individual strain components.

Two sets of rheological coefficients for the Burgers-Humphrey model are available so far, either of which may be used as input data for the simulation. The first was measured by Ren (1991) on fiber materials and fitted to equations by Haselein (1998). The second set has been derived from data presented by von Haas (1998) for fiber, particle, and strand materials; those coefficients for fiber materials will be used for the simulation run presented in this paper.

Numerical procedure and model implementation

The heat and mass transfer model described above consists of a set of constitutive flux

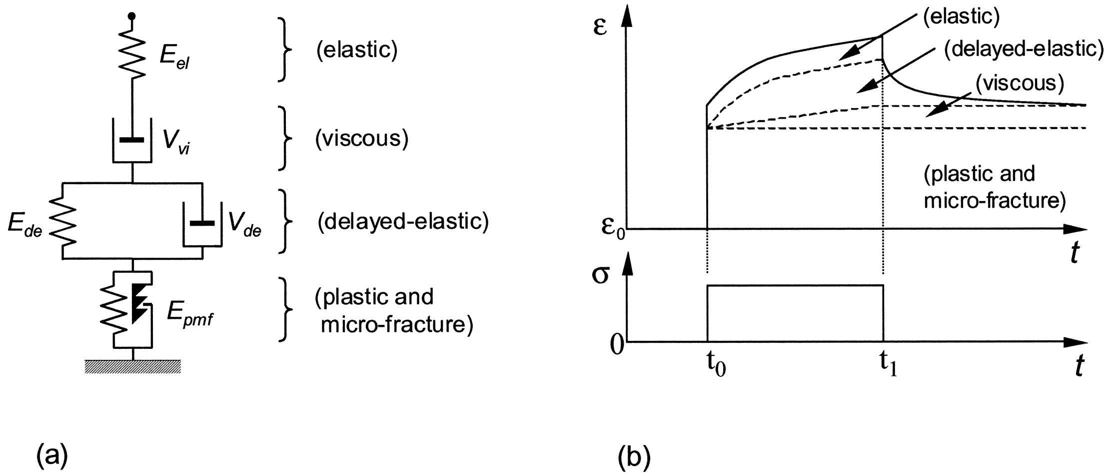

FIG. 1. (a) Five-element Burgers-Humphrey model, representing four strain components. E = modulus of elasticity, V = viscosity, E_{pmf} = coefficient for plastic and micro-fracture element. The non-linear behavior of each element is not symbolized in this schematic. Refined after Ren (1991). (b) The four strain components described by the Burgers-Humphrey model as a function of stress σ and time t. ϵ = strain.

equations (Eqs. (1), (2) and (4)) that are coupled by local energy and mass balances. Following this approach, the derivation of heat and mass conservation equations and their subsequent discretization was obviated.

The wood-furnish mat to be modelled is subdivided into finite-differencing control regions. Computations for each time step include three distinct consecutive procedures. First, heat and mass fluxes between the midpoints of adjacent control regions are calculated under steady-state conditions to determine the diffusant quantities (e.g., energy) flowing across the interfaces between neighboring regions. Second, knowing gains and losses of the diffusant within each control region, new values for the state variables (e.g., temperature) are calculated. Finally, the state variables are corrected for compression or expansion of the control regions. To improve the efficiency of computations, an adaptive time step scheme in combination with a mechanistic implicit approach for the cross-sectional convective flow calculations was adopted. The in-house programming code for the simulation program is written in ANSI C.

MODELING THE CONTINUOUS PRESS

Characteristics of the continuous pressing process

The earliest continuously working hot press for particleboard, the so-called Bartrev press, was developed during the 1950s in England. This first generation of continuous press was not, however, very successful. New technologies developed during the 1970s and 1980s led to today's continuous presses that are larger and more effective. Such presses for medium density fiberboard (MDF) typically have a production width of 2.10 to 3.15 m, press lengths up to 50 m, and production capacities as great as 280,000 m^3 per year (from data published by Sunds Defibrator 1998).

The adhesive-treated wood-furnish mat is conveyed horizontally through the press between two endless steel belts. For mat densification and adhesive cure, heat and pressure have to be transferred into the moving mat. A simplified representation of the vertical cross-sectional structure of the press in the feed direction is given in Fig. 2. The rolling elements (usually steel rods or roller carpets), located between the heating platens and the endless

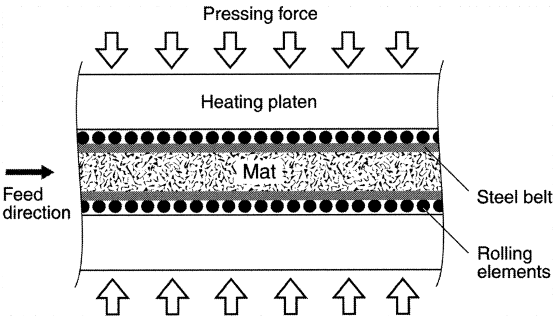

FIG. 2. A cross-section of the center zone of a typical continuous press.

steel belts, are important components for heat and pressure transfer into the mat. The rolling elements allow almost frictionless movement of the mat through the press. Isobaric approaches where heat and pressure are transferred by way of a thin oil film, as used in coating presses, to date have proven inappropriate for wood-based composite production.

Pressing frames typically are arranged in series over the length of the press. For each frame, the vertical position (i.e., distance between steel belts) or the pressing pressure is controllable within limits that are dictated by the vertical position in the two neighboring frames. Hence, a thickness or pressure profile over the length of the press can be established. In addition, it is usually possible to vary the mat thickness over the width of the press for some of the frames.

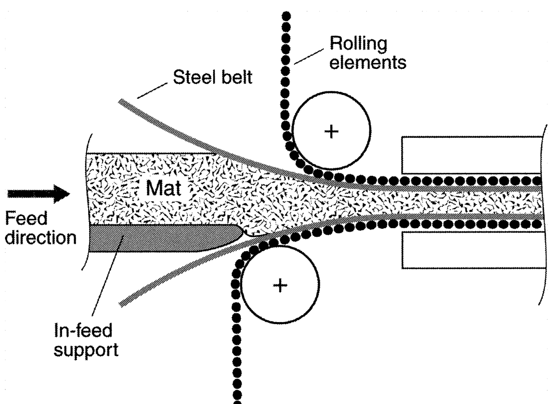

FIG. 3. Example of an in-feed section for a typical continuous press.

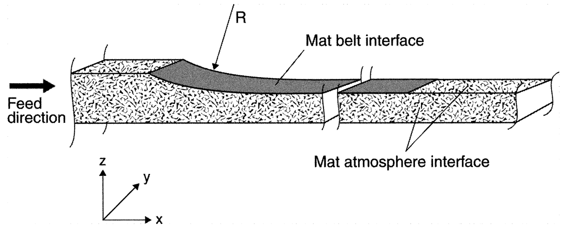

FIG. 4. Schematic of the model boundaries. R = in-feed radius.

The heating platens are divided longitudinally into zones. Usually, the temperatures in these zones decrease towards the press outlet. Since the rolling elements and the steel belts move through the press with the mat, heat not only migrates vertically into the mat, but also is conveyed horizontally in the feed direction. This horizontal 'dragging' of heat, together with the complexity of describing heat transfer through the rolling elements, makes it difficult to accurately infer steel belt temperatures from known platen temperatures.

The geometry, technical details, and controlling strategies of the in-feed section where the mat enters the press depend on the press manufacturer. A typical in-feed section is depicted in Fig. 3. A large proportion of the total mat densification occurs in this part of the press, and the rapid compression of the water vapor-air mixture inside the mat creates a significant back-flow of the gas counter to the feed direction. Usually the shape of the in-feed section is adjustable up to a certain degree. Changing this shape allows manipulation of the gas back-flow, as well as mechanisms that ultimately dictate the product's density profile.

System boundaries

Press designs vary among press manufacturers. In order to provide a model that may be used to describe a wide range of different press designs and methods of operation, a rather adaptable formulation of the boundary conditions with relatively straightforward geometries has been developed.

The scheme of the mat used in the present model is shown in Fig. 4. The horizontal surfaces of the mat are the upper and lower model boundaries. The lower surface follows a flat plane; the shape of the upper steel belt can be specified (position control). Alternatively, a longitudinal pressure profile can be used as the input data (load control). The upper and lower steel belts contact the mat (at the press entry) or leave it (at the outlet) at the same horizontal positions. The shape of the upper steel belt in the in-feed section is specified by the in-feed radius *R*. Consequently, only position control is possible in the in-feed section.

Both horizontal mat surfaces are sealed against gas escape within the press and are assumed to be open to the ambient atmosphere in front of and behind the press. Although the mat may lie on an impermeable conveyer belt before entering the press, the gap between conveyer belt and steel belt at the press entry justifies the assumption of gas escape through the lower surface. The edges of the mat are open to the ambient atmosphere.

The difficulty of inferring steel belt temperature from heating platen temperature has already been mentioned. Belt temperature distribution in the feed direction is therefore directly defined as a boundary condition. It has been assumed that the mat surface temperature is equal to that of the steel belt.

At the mat surfaces in front of and behind the press and at the edges of the mat, almost all heat transfer is due to the escape of vapor and air. The importance of conductive heat transfer at these boundaries is likely to be minor and therefore was not considered.

Strategy for continuous press modeling

Whereas hot pressing in a batch press represents an unsteady-state type of problem, continuous pressing can be described as a steady-state process if the press is the reference system. However, if the moving wood-furnish mat rather than the press is the reference system, the process must be treated as an unsteady-state type of problem. After careful consideration, the latter approach was selected for use here.

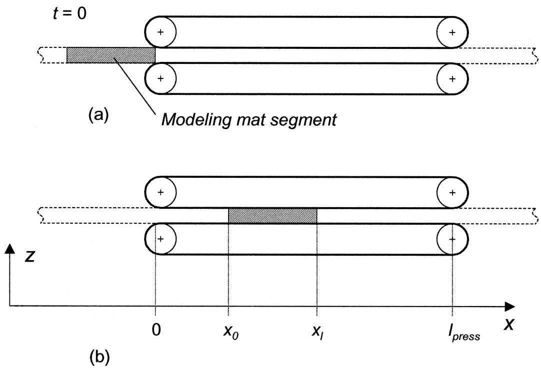

FIG. 5. Schematic of the modeling mat segment passing through the continuous press: (a) beginning of simulation; (b) mat segment within press. x_0 = position of left boundary, x_l = position of right boundary, l_{press} is position of last mat-steel belt contact.

In order to model the endless mat moving through the press, a segment of finite length in the feed direction is considered (Fig. 5). Choosing such an approach, the number of modeling subdivisions in the feed direction could be kept at a manageable number while achieving a satisfactory level of accuracy, particularly at the mouth and exit zone of the press where gradients are steep. The simulation starts before the mat segment enters the press and ends after it has left. During each time step, Δt, the segment moves forward by the small distance $\Delta x = v \cdot \Delta t$, where v is the feed speed. Heat and mass transfer and rheology are computed for the modeling mat segment as described above. The basic idea of this approach is that only the boundary conditions differ from those of a batch press; the body to be modeled and the description of the physical mechanisms are the same for both continuous and batch presses.

The two boundaries in the y-z plane (perpendicular to the feed direction) require some attention. Such boundaries can be treated either as open or as closed to gaseous flow. Both choices are extreme situations and do not reflect reality; inaccuracies are inevitable. Towards the central y-z plane (i.e., half way between these two boundaries), the inaccuracies decline. Therefore, the ratio of length to width

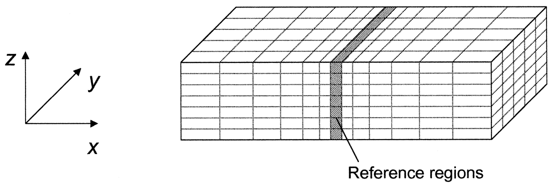

FIG. 6. Modeling mat segment with grid clustered around reference regions.

of the modeling mat segment must be big enough so that the inaccuracies at the boundaries do not affect the central y-z plane. Trial runs showed that the effect of the boundaries in the y-z plane is negligible for length-to-width ratios larger than five. The control regions in the central y-z plane are named 'reference regions' (Fig. 6). These regions are monitored while the mat moves through the press, and results for these regions are recorded.

Another source of inaccuracy that must be considered is the discontinuity in the boundary conditions where the steel belt first contacts the mat (press entry) and leaves the mat (outlet). A control region adjacent to the horizontal boundary is treated as open to the ambient atmosphere as long as the center of the region is outside the press. Once the center of the region has passed the mat-steel belt contact point, it is assumed that the surface of the control region is entirely covered by the steel belt. The resolution and, therefore, the accuracy improve with greater narrowness of the grid in the x-direction at these particular positions. On the other hand, in order to avoid unacceptably long execution times, the length of the grid cells cannot be infinitely small. Clustering the regions in the x-direction around the reference regions, as shown in Fig. 6, minimizes the error caused by the discontinuity in the boundary condition while keeping the number of control regions reasonably small. This approach was justified by test runs with different grid schemes. Other grid schemes may also be specified for simulation runs.

A SIMULATION EXAMPLE

Initial and boundary conditions for the simulation run presented below were chosen to

TABLE 1. *Input conditions for the model demonstration simulation run.*

Condition	Value
Material	MDF fiber
Mat width	2.30 m
Height of pre-compressed mat	160 mm
Density of pre-compressed mat	100 kg/m^3
Initial mat temperature	40°C
Initial moisture content	9.6%
Radius of in-feed section	30 m
Feed speed	129 mm/s

correspond with the industrial press used by Steffen et al. (1999)[1] to make temperature and gas pressure measurements during pressing.

Specification of input conditions

Key input specifications are listed in Table 1 and Fig. 7. A one-layered MDF mat with homogeneous initial conditions was modeled. Target thickness and density were about 20 mm and 800 kg/m^3, respectively. However, because load control was adopted, the actual final panel thickness and density were a consequence of the specified mat and pressing conditions.

The steel belt temperature was needed as a boundary condition. Neither the temperatures recorded for the heating platens nor the temperature measured near the surface of the mat

[1] A more complete presentation of the results of these measurements can be found in Thoemen (2000).

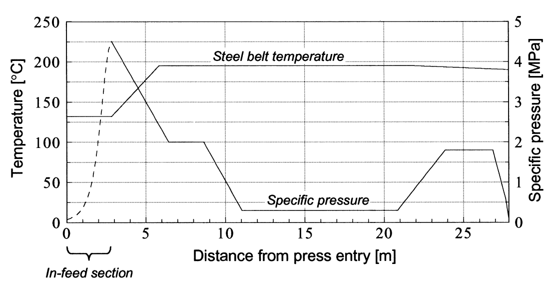

FIG. 7. Specified pressing pressure and steel belt temperature for the model demonstration simulation run. In the in-feed section, the pressing pressure cannot be defined directly, but is dictated by the radius and absolute level of the upper steel belt.

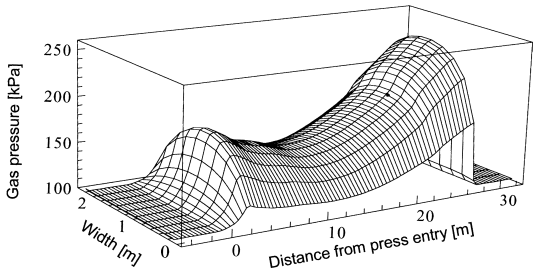

FIG. 8. Predicted total gas pressure distribution within the central layer of the mat. Gas pressures are given as absolute values.

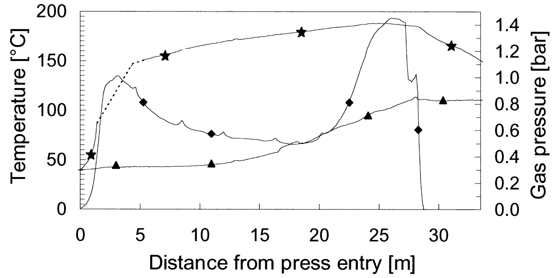

FIG. 9. Core gas pressures (♦) and temperatures (★—surface, ▲—core) measured in an MDF mat as it passes through the 28 m industrial press corresponding to the presented model data (from Steffen et al. 1999).

(Steffen et al. 1999) represent the exact steel belt temperature. In the absence of reliable industrial data, the longitudinal temperature profile (Fig. 7) was estimated. This estimate is based on the steel belt temperature measured right in front of the press entry (132°C) and the temperature measured near the surface of the mat.

A 10-meter long mat segment was considered for modeling purposes. The mat was assumed to be symmetrical along the width and the thickness, so that calculations were done for only one fourth of the mat. A modeling grid of 15 × 5 × 10 control regions (x, y, z) was used, and the control regions were clustered in the feed direction around the reference regions (Fig. 6). The size ratio of outermost to innermost regions was seven. All results are plotted for the reference regions, i.e., half way between the two boundaries perpendicular to the feed direction. The simulation run was executed with a specified minimum of 500 time steps per second.

Model predictions

Gas pressure predictions.—More than 95% of the total gas pressure in the uncompressed mat before it enters the press can be attributed to air in the vapor-air mixture. The fast compression of the air leads to a predicted total gas pressure maximum about 75 kPa above atmospheric pressure early in the pressing cycle (Fig. 8). During the subsequent period of the pressing cycle, when the mat thickness stays almost constant, some of the gas entrapped inside the mat escapes through the edges; the gas pressure in the center slowly drops to an intermediate minimum of about 40 kPa above ambient. This relatively high level of the first maximum and the subsequent intermediate minimum corresponds well in trend with the gas readings made on a corresponding industrial press (Fig. 9). Details of the measurement methods are to be found in Steffen et al. (1999).

Towards the end of the press, total gas pressure rises considerably. The generation of water vapor, together with the compression of the gas during the second densification step near the end of the press, causes the final gas pressure to reach a maximum of almost 150 kPa above atmospheric pressure right before the panel leaves the press. Throughout the entire pressing process, a near-parabolic gas pressure distribution is generated across the width of the mat.

Figure 10 shows the core layer distribution of total gas pressure for the first 6 m of the press. The arrows represent the horizontal gas velocity in the central layer, defined as the volumetric gas flow/sec/unit cross-sectional area.[2] The gas pressure maximum is reached three meters into the press, in the middle of the mat. Most of the vapor-air mixture escapes through the edges in the in-feed section and through

[2] The contact points of the mesh lines in Fig. 8 and the vector bases in Fig. 10 represent the centers of the grid regions. Hence, the first and last plotted values over the width represent the values 5% from the actual mat edge.

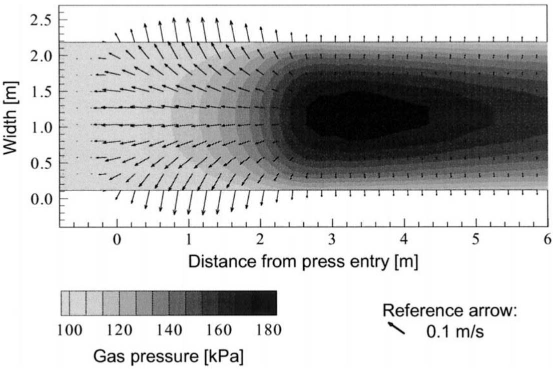

FIG. 10. Predicted total gas pressure distribution and gas velocities (arrows) for the first 6 m within the central layer of the mat. Gas pressures are given as absolute values.

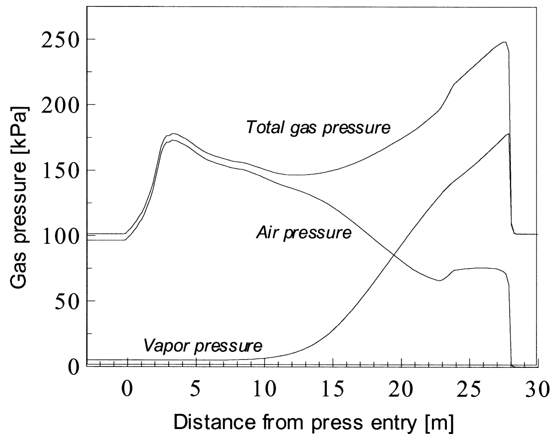

FIG. 11. Predicted total gas pressure, vapor pressure and air pressure in the middle of the central plane of the mat.

the surfaces right before the mat enters the press. The magnitude of such gas counter-flow may be of practical importance because it can disrupt the surface of the loosely packed mat.

The partition of predicted total gas pressure between water vapor and air for the middle of the central plane of the mat is shown as Fig. 11. The vapor pressure in the center starts to rise once the mat is about one third into the press, gradually replacing the air from this mat layer. However, the predictions also indicate that not all of the air will be driven out of the mat during pressing; a considerable quantity of air may still exist in the core at the end of the pressing cycle. This simulation result is supported by the measurements shown in Fig. 9; core temperature and absolute gas pressure reached 114°C and 230 kPa, respectively, immediately before the mat left the press. The water vapor saturation pressure at 114°C is, however, only 164 kPa. The difference between measured gas pressure and actual vapor pressure, which cannot exceed the saturation pressure, must be mainly due to air.

Temperature predictions.—The predicted temperature distribution at four individual cross-sectional positions is displayed in Fig. 12. The zones of condensation and evaporation progressing from the two surfaces towards the central plane of the mat cause the typical shape of the temperature line shown for the intermediate layer $z = 4$ (there are ten subdivisions in the half-thickness.) Main features of this line include a time lag before the temperature begins to rise and a temperature plateau near, but not equal to, 100°C. The temperature plateau of 113°C for this layer is much higher than the temperatures observed in laboratory (e.g., Gefahrt 1977) or in industrial particleboard batch presses (e.g., Humphrey and Bolton 1989b). Model predictions suggest that the relative humidity (not displayed here) in the intermediate layers exceeds 90% during the stage of the temperature plateau. The temperature at such near-saturation conditions is closely linked to the prevailing vapor pressure. Evidently, the high predicted-temperature plateau results from the relatively

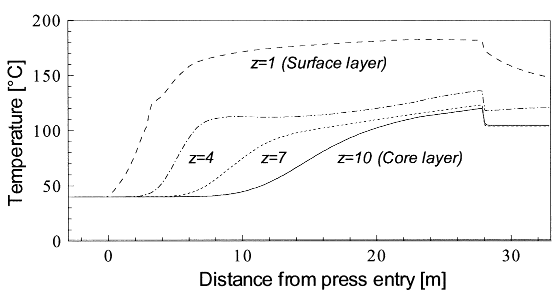

FIG. 12. Predicted temperature distribution at four cross-sectional positions within the central x-z plane of the mat.

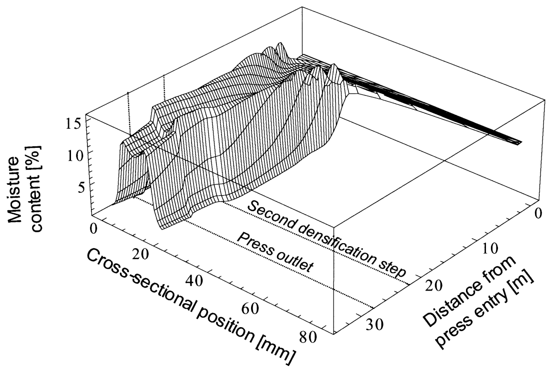

FIG. 13. Predicted moisture distribution within the central x-z plane of the mat.

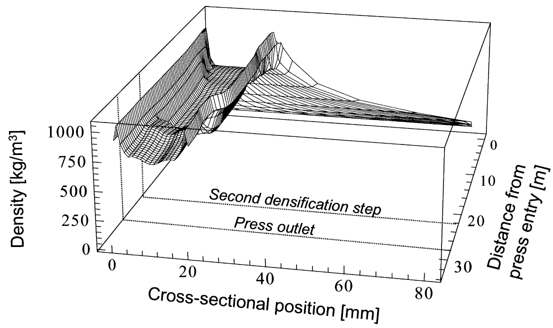

FIG. 14. Predicted density profile development within the central x-z plane of the mat.

high gas pressure (Fig. 8). Predicted core temperature distributions agree well with those measured in the industrial continuous press (Fig. 9).

Moisture content predictions.—Figure 13 displays the development of the cross-sectional moisture profile. The MC in the surface layers declines soon after the mat has entered the press and then stays relatively low. Moisture rises towards a maximum in the intermediate locations between mat surfaces and central plane before dropping again. The position of maximal MC thus continuously moves forward towards the core. In the simulation presented here, the moisture maxima do not reach the core throughout the entire process, but this prediction should not be generalized. Under different circumstances, the final moisture maximum may well lay in the core of the mat.

A pronounced moisture drop is predicted when the panel leaves the press. The magnitude of this drop suggests that it is not only vapor already in existence within the voids of the mat that is lost; bound water must also be changing phase and subsequently escaping. In fact, water evaporates rapidly because of changes of the thermodynamic conditions at the press outlet. This rapid evaporation causes the moisture drop, as well as the temperature drop displayed in Fig. 12. Because the strength of partially or fully cured adhesive bonds depends on temperature, such temperature drops may be important. These issues and their significance are developed further by Humphrey (1997) and Kim (2003).

Density profile predictions.—Development of density profiles during continuous pressing depends on the longitudinal distribution of pressing pressure in concert with the spatial distribution of rheological mat properties. These mat properties are determined by temperature, MC and density; they change considerably throughout the pressing process. Furthermore, an impact of the adhesive cure on the mat properties may be expected. However, since the effect of adhesive cure on rheological mechanisms is not considered in the present modeling approach, the following interpretations are based only upon those explanations that can be derived from the present form of the Burgers-Humphrey model. Inclusion of adhesive effects on mats' rheological properties is presently being addressed. Preliminary predictions of adhesive bond strength development within the mat using adhesive bonding kinetics data measured using the Automated Bonding Evaluation System (ABES) approach (Humphrey 1999), are to be found in Humphrey and Thoemen (2000).

During the main densification in the first section of the press, high densities are formed near the surfaces of the mat, while the densities of the inner layers remain relatively low (Fig. 14). The high surface densities result from softening during and right after the main densification. Because of the viscous-elastic component of the material's rheological characteristics, the mat expands again somewhat during the following stage of low pressure.

If no further densification were to take place, the density profile of the final panel would be relatively simple, with high densities near but not at the surfaces and a near-flat density distribution across the core. However, as specified for the simulation, the mat sustains further densification in a second step near the end of the press. At this stage, the cross-sectional distributions of rheological properties differ greatly from those near the press entry. Densification is greatest in the layers midway between surface and core, but almost no densification occurs in the surface layers. A rather complex density profile is thereby generated, with intermediate density peaks in the former layers. Such intermediate density peaks have been measured frequently (e.g., Wang et al. 2000). After leaving the press, the panel relaxes, leading to a predicted spring-back of about 4%. The core regions contribute most to this spring-back, whereas the surface layers do not expand significantly. The final panel thickness is 20.4 mm.

CONCLUSIONS

The model presented in this paper is directly applicable to continuous presses. It accounts for those features that are specific to this press type, including changing mat thickness and steel belt temperatures in the feed direction, and the escape of vapor and air through the horizontal surfaces immediately in front of and behind the press. Additional characteristics of continuous presses, such as the possibility to vary the mat thickness across the width of the press, are easy to incorporate into the existing model.

The main purpose of this paper was to describe the strategy developed and implemented to simulate continuous presses, and to illustrate the potential of the model by displaying and discussing results of just one simulation run. Clearly, the results presented cover only a small fraction of the range of possibilities. All variables included in the model may be output and displayed for any location, and the model may be run with a diversity of raw material and process configurations. Exploration of gas flow and heat transfer patterns, as well as sensitivity studies, will improve our knowledge of the process. Such analysis will be presented in future publications.

ACKNOWLEDGMENTS

The authors are grateful to G. Siempelkamp GmbH & Co. for facillitating our access to continuous presses for study. This work was supported by USDA funds through the Center for Wood Utilization at Oregon State University and by the Federal Ministry of Economics and Technology (Germany) through the German Wood Research Foundation (DGfH). The authors also acknowledge the encouragement of Drs. A. Fruehwald and A. Steffen.

REFERENCES

BOLTON, A. J., AND P. E. HUMPHREY. 1988. The hot pressing of dry-formed wood-based composites. Part I. A review of the literature, identifying the primary physical processes and the nature of their interaction. Holzforschung 42:403–406.

DENISOV, O. B., P. P. ANISOV, AND P. E. ZUBAN. 1975. Untersuchung der Permeabilität von Spanvliesen. Holztechnologie 16(1):10–14.

ENGELHARDT, F. 1979. Untersuchungen über die Wasserdampfsorption durch Buchenholz im Temperaturbereich von 110°C bis 170°C. Holz Roh- Werkst. 37:99–112.

GEFAHRT, J. 1977. Zur Spänevorwärmung mit Hochfrequenzenergie—Modell zur Berech-nung des Temperaturverlaufes in Vliesmitte bei der Heißpressung. Holz Roh-Werkst. 35:183–188.

HASELEIN, C. R. 1998. Numerical simulation of pressing wood-fiber composites. Ph.D. thesis, Oregon State Univ., Corvallis, OR. 244 pp.

HUMPHREY, P. E. 1997. Thermoplastic characteristics of partially cured thermosetting-to-wood bonds. Pages 366–373 *in* Kajita and Tsunoda, eds. Proc. Third Pacific Rim Bio-Based Composites Symp., Kyoto, Japan. Wood Research Inst., Kyoto, Japan.

———. 1999. Bonding speed of adhesives: an automated evaluation system. Pages 139–146 *in* M. Wolcott, ed. Proc. 33rd International Particleboard and Composite Materials Symp., Washington State Univ., Pullman, WA.

———, AND A. J. BOLTON. 1989a. The hot pressing of dry-formed wood-based composites. Part II. A simulation model for heat and moisture transfer. Holzforschung 43(3):199–206.

———, AND A. J. BOLTON. 1989b. The hot pressing of dry-formed wood-based composites. Part VI. The importance of stresses in the compressed mattress and their relevance to the minimization of pressing time, and the variability of board properties. Holzforschung 43(6): 406–410.

———, AND H. THOEMEN. 2000. The continuous pressing of wood-based panels: a simulation model, input data and typical results. Pages 303–311 *in* P. D. Evans, ed. Proc. Pacific Rim BioBased Composites Symp. Canberra, Australia. Australia National University.

KAVVOURAS, P. K. 1977. Fundamental process variables in particleboard manufacture. Ph.D. thesis, Univ. of Wales, UK. 156 pp.

KIM, J-W. 2003. Gas injection consolidation of miniature natural fiber beams. Ph.D. thesis, Oregon State Univ., Corvallis, OR. 219 pp.

REN, S. 1991. Thermo-hygro rheological behavior of materials used in the manufacture of wood-based composites. Ph.D. thesis, Oregon State Univ., Corvallis, OR. 226 pp.

STEFFEN, A., G. VON HAAS, A. RAPP, P. E. HUMPHREY, AND H. THÖMEN. 1999. Temperature and gas pressure in MDF-mats during industrial continuous hot pressing. Holz Roh-Werkst. 57:154–155.

THOEMEN, H. 2000. Modeling the physical processes in natural fiber composites during batch and continuous pressing. Ph.D. thesis, Oregon State Univ., Corvallis, OR. 187 pp.

———, AND P. E. HUMPHREY. 2003a. The physical processes relevant during hot pressing of wood-based composites. Part I. Model description: Mass and heat transfer. In preparation.

———, AND ———. 2003b. The physical processes relevant during hot pressing of wood-based composites. Part II. Model description: Rheology. In preparation.

VON HAAS, G. 1998. Untersuchungen zur Heißpressung von Holzwerkstoffmatten unter besonderer Berücksichtigung des Verdichtungsverhaltens, der Permeabilität, der Temperaturleitfähigkeit und der Sorptionsgeschwindigkeit. Dissertation, Univ. of Hamburg, Germany. 264 pp.

WANG, S., P. M. WINISTORFER, W. W. MOSCHLER, AND C. HELTON. 2000. Hot-pressing of oriented strandboard by step-closure. Forest Prod. J. 50(3):28–34.

WEICHERT, L. 1963. Untersuchungen Uber das Sorptions- und Quellungsverhalten von Fichte, Buche und Buchen-Preissvollholz bei Temperaturen zwischen 20°C und 100°C. Holz Roh- Werkst. 21:290–300.